Electronic supplementary information on **Optical deformation potential and self-trapped excitons in 2D hybrid perovskites**

zhi-gang.yu@wsu.edu

August 28, 2019

Contents

1 Exciton states in HOIPs

An exciton consists of an electron in the conduction band and a hole in the valence band. According to the newly developed effective-mass theory, the conduction- and valence-band basis functions for both 3D[1] and 2D HOIPs[2] can be expressed in terms of Pb 6s orbital denoted S and 6p orbitals denoted X, Y, and Z,

$$\mathrm{v}_{+(-)} = S\uparrow(\downarrow), \tag{1}$$

$$\mathrm{c}_{+(-)} = +(-)\frac{\cos\xi}{\sqrt{2}}[X-(+)iY]\uparrow(\downarrow)-\sin\xi Z\downarrow(\uparrow), \tag{2}$$

where $\tan 2\xi = \frac{2\sqrt{2}\lambda}{\lambda-3\delta}$ with λ and δ charactering the spin-orbit coupling (SOC) and crystal-field splitting. The angular momentum is $s=1/2$ for the valence band $\mathrm{v}_{\pm}$, and $j=1/2$ ($\boldsymbol{j}=\boldsymbol{l}+\boldsymbol{s}$ with $l=1$ and $s=1/2$)

for the first conduction band $c_\pm$. Denoting a hole in the valence band as $\bar{v}_\pm$ (time reversal of $v_\pm$), we characterize exciton wavefunctions of HOIPs via representations of the C_4 group[1],

$$\begin{aligned}
\Gamma_1 &= \frac{1}{\sqrt{2}}(c_+\bar{v}_- - c_-\bar{v}_+) \\
&= -\frac{1}{2}\cos\xi(X+iY)S\downarrow_e\downarrow_h + \frac{1}{2}\cos\xi(X-iY)S\uparrow_e\uparrow_h - \frac{1}{2}\sin\xi ZS(\uparrow_e\downarrow_h + \downarrow_e\uparrow_h), \quad (3)\\
\Gamma_2 &= \frac{1}{\sqrt{2}}(c_+\bar{v}_- + c_-\bar{v}_+) \\
&= -\frac{1}{2}\cos\xi(X+iY)S\downarrow_e\downarrow_h - \frac{1}{2}\cos\xi(X-iY)S\uparrow_e\uparrow_h - \frac{1}{2}\sin\xi ZS(\uparrow_e\downarrow_h - \downarrow_e\uparrow_h), \quad (4)\\
\Gamma_5^+ &= c_+\bar{v}_+ = -\frac{1}{\sqrt{2}}\cos\xi(X+iY)S\downarrow_e\uparrow_h - \sin\xi ZS\uparrow_e\uparrow_h, \quad (5)\\
\Gamma_5^- &= c_-\bar{v}_- = -\frac{1}{\sqrt{2}}\cos\xi(X-iY)S\uparrow_e\downarrow_h + \sin\xi ZS\downarrow_e\downarrow_h\,. \quad (6)
\end{aligned}$$

2 Optical selection rules

The optical selection rules of these exciton states can be derived from the matrix elements of the momentum operator, $\boldsymbol{e}\cdot\boldsymbol{p}$ with $\boldsymbol{e}$ being the electric-field polarization of the electromagnetic wave. According to the effective-mass model[1], we have

$$\begin{aligned}
\langle\Gamma_1|\boldsymbol{e}\cdot\boldsymbol{p}|\mathrm{G}\rangle &= 0, \quad (7)\\
\langle\Gamma_2|\boldsymbol{e}\cdot\boldsymbol{p}|\mathrm{G}\rangle &= i\frac{m}{\hbar}\sin\xi P_\parallel \boldsymbol{e}_z \quad (8)\\
\langle\Gamma_5^\pm|\boldsymbol{e}\cdot\boldsymbol{p}|\mathrm{G}\rangle &= i\frac{m}{\hbar}\cos\xi P_\perp \boldsymbol{e}_\pm \quad (9)
\end{aligned}$$

where m is the free-electron mass, and $P_\parallel$ and $P_\perp$ are the Kane parameters. Hence Γ_1 is dark, Γ_2 absorbs light polarized along the z-axis, and doublet $\Gamma_5^\pm$ absorbs light polarized in the x-y plane.

3 Derivation of Eq. (2) in the main text

The polar coupling of electrons and electron-hole pairs in HOIPs have been examined in Refs.[3,4], and can be expressed as

$$H_\mathrm{p}^\mathrm{e} = i\sum_{\boldsymbol{q}}\left(\frac{4\pi\alpha_\mathrm{e}}{\mathscr{V}}\right)^{1/2}\frac{\hbar\Omega_\mathrm{s}}{q}\left(\frac{\hbar}{2m_\mathrm{e}\Omega_\mathrm{s}}\right)^{1/4}(b_{\boldsymbol{q}}e^{i\boldsymbol{q}\cdot\boldsymbol{r}_\mathrm{e}} - b_{\boldsymbol{q}}^\dagger e^{-i\boldsymbol{q}\cdot\boldsymbol{r}_\mathrm{e}}), \quad (10)$$

for electron and

$$H_\mathrm{p}^\mathrm{h} = -i\sum_{\boldsymbol{q}}\left(\frac{4\pi\alpha_\mathrm{h}}{\mathscr{V}}\right)^{1/2}\frac{\hbar\Omega_\mathrm{s}}{q}\left(\frac{\hbar}{2m_\mathrm{h}\Omega_\mathrm{s}}\right)^{1/4}(b_{\boldsymbol{q}}e^{i\boldsymbol{q}\cdot\boldsymbol{r}_\mathrm{h}} - b_{\boldsymbol{q}}^\dagger e^{-i\boldsymbol{q}\cdot\boldsymbol{r}_\mathrm{h}}), \quad (11)$$

for hole. Here $\alpha_\mathrm{e}/\alpha_\mathrm{h} = \sqrt{m_\mathrm{e}/m_\mathrm{h}}$, and $\boldsymbol{r}_e$ and $\boldsymbol{r}_h$ are electron and hole coordinates, which are related to the center-of-mass and relative coordinates $\boldsymbol{R}$ and $\boldsymbol{r}$ via $\boldsymbol{r}_e = \boldsymbol{R} + p_\mathrm{e}\boldsymbol{r}$ and $\boldsymbol{r}_h = \boldsymbol{R} - p_\mathrm{h}\boldsymbol{r}$. The polar coupling of an exciton is then $H_\mathrm{p}^\mathrm{ex} = H_\mathrm{p}^\mathrm{e} + H_\mathrm{p}^\mathrm{h}$, whose matrix elements between excitons with wave vectors $\boldsymbol{k}$ and $\boldsymbol{k}-\boldsymbol{q}$ is[5]

$$\langle\Phi_{\boldsymbol{k}}|H_\mathrm{p}^\mathrm{ex}|\Phi_{\boldsymbol{k}-\boldsymbol{q}}\rangle = V_\mathrm{p}^\mathrm{ex}(\boldsymbol{q})(b_{\boldsymbol{q}} + b_{\boldsymbol{q}}^\dagger), \quad (12)$$

$$
\begin{aligned}
V_{\rm p}^{\rm ex}(\boldsymbol{q}) &= \int d^3r\Big(\frac{1}{\pi a_0^3}\Big)^2 e^{-2r/a_0}\frac{W}{q}\Big(e^{ip_{\rm e}\boldsymbol{q}\cdot\boldsymbol{r}}-e^{-ip_{\rm h}\boldsymbol{q}\cdot\boldsymbol{r}}\Big)\\
&= \frac{W}{q}\Big(\frac{1}{[1+(p_{\rm e}a_0q/2)^2]^2}-\frac{1}{[1+(p_{\rm h}a_0q/2)^2]^2}\Big),
\end{aligned}
\tag{13}
$$

with $W = i(4\pi\alpha_{\rm e}/\mathscr{V})^{1/2}\hbar\Omega_{\rm s}$.

4 Exciton bandwidths

The hopping t_{ij} in Hamiltonian (4) of the main text is due ultimately to the Coulomb interaction[5]

$$
V(\boldsymbol{r}_i-\boldsymbol{r}_j) = \frac{e^2}{|\boldsymbol{r}_i-\boldsymbol{r}_j|},
\tag{14}
$$

between electrons located at $\boldsymbol{r}_i$ and $\boldsymbol{r}_j$. Electron $\boldsymbol{r}_i$ can be expressed as $\boldsymbol{r}_i = \boldsymbol{\rho}_i+\boldsymbol{R}_i$, with $\boldsymbol{R}_i$ being the location of site i. Since a tightly bound exciton in 2D HOIPs can be regarded as localized at a single PbX_6 octahedron, its wavefunction can be approximately expressed as $\tilde{\Phi}_i(\boldsymbol{r}_i) = \phi_c^*(\boldsymbol{r}_i)\phi_v(\boldsymbol{r}_i)$, and t_{ij} is then

$$
\begin{aligned}
t_{ij} &= \frac{1}{2}\langle\tilde{\Phi}_i|V(\boldsymbol{r}_i-\boldsymbol{r}_j)|\tilde{\Phi}_j\rangle\\
&= \frac{1}{2}\int\phi_c^*(\boldsymbol{r}_i)\phi_v(\boldsymbol{r}_i)V(\boldsymbol{r}_i-\boldsymbol{r}_j)\phi_v^*(\boldsymbol{r}_j)\phi_c(\boldsymbol{r}_j)d^3r_id^3r_j,
\end{aligned}
\tag{15}
$$

Since $\phi_{c(v)}(\boldsymbol{r})$ is highly localized, we can expand the Coulomb potential

$$
V(\boldsymbol{r}_i-\boldsymbol{r}_j) = \frac{e^2}{|\boldsymbol{R}_{ij}|}+(\boldsymbol{\rho}_i-\boldsymbol{\rho}_j)\cdot\nabla V(\boldsymbol{R}_{ij})+\frac{1}{2}(\boldsymbol{\rho}_i-\boldsymbol{\rho}_j)(\boldsymbol{\rho}_i-\boldsymbol{\rho}_j):\nabla\nabla V(\boldsymbol{R}_{ij})+\ldots
\tag{16}
$$

The contribution from the first term is zero because the conduction and valence wave functions are orthogonal, $\int d^3r_i\phi_c^*(\boldsymbol{r}_i)\phi_v(\boldsymbol{r}_i)\to 0$. The first finite contribution to t_{ij} comes from the third terms in Eq. (16),

$$
t_{ij} = \frac{\boldsymbol{d}_i\cdot\boldsymbol{d}_j^*}{|\boldsymbol{R}_{ji}|^3}-3\frac{(\boldsymbol{d}_i\cdot\boldsymbol{R}_{ji})(\boldsymbol{d}_j^*\cdot\boldsymbol{R}_{ji})}{|\boldsymbol{R}_{ji}|^5},
\tag{17}
$$

where

$$
\boldsymbol{d}_i = \int d^3\rho_i\phi_c^*(\boldsymbol{\rho}_i)e\boldsymbol{r}_i\phi_v(\boldsymbol{\rho}_i).
\tag{18}
$$

For the Γ_5 excitons, the transition dipole is

$$
\boldsymbol{d}_\pm = \langle\Gamma_5^\pm|e\boldsymbol{e}\cdot\boldsymbol{r}|{\rm G}\rangle = -i\frac{e\hbar}{mE_{\rm g}}\langle\Gamma_5^\pm|\boldsymbol{e}\cdot\boldsymbol{p}|{\rm G}\rangle.
\tag{19}
$$

Since the oscillator strength from Γ_5 is defined as[5]

$$
f_\pm = \frac{2}{mE_{\rm g}}|\langle\Gamma_5^\pm|\boldsymbol{e}\cdot\boldsymbol{p}|{\rm G}\rangle|^2 = \frac{2mP_\perp^2\cos^2\xi}{\hbar^2E_{\rm g}},
\tag{20}
$$

the transition dipole associated with $\Gamma_5^\pm$ excitons is

$$
\boldsymbol{d}_\pm = d_0\boldsymbol{e}_\pm,\ d_0 = \frac{e\hbar}{mE_{\rm g}}\sqrt{f_\pm}
\tag{21}
$$

Since the dipole-dipole interaction decays with distance rapidly, we consider only the nearest neighbor coupling. If we denote the nearest-neighboring coupling of the tetragonal structure as t_q ($q = x, y, z$), for $\boldsymbol{d} = d_0 \boldsymbol{e}_+$,

$$t_x = \frac{\boldsymbol{d}\cdot\boldsymbol{d}^*}{a^3} - 3\frac{(\boldsymbol{d}\cdot\boldsymbol{e}_x)(\boldsymbol{d}^*\cdot\boldsymbol{e}_x)}{a^3} = -\frac{d_0^2}{2a^3}, \tag{22}$$

$$t_y = \frac{\boldsymbol{d}\cdot\boldsymbol{d}^*}{a^3} - 3\frac{(\boldsymbol{d}\cdot\boldsymbol{e}_y)(\boldsymbol{d}^*\cdot\boldsymbol{e}_y)}{a^3} = -\frac{d_0^2}{2a^3}, \tag{23}$$

$$t_z = \frac{\boldsymbol{d}\cdot\boldsymbol{d}^*}{c^3} - 3\frac{(\boldsymbol{d}\cdot\boldsymbol{e}_z)(\boldsymbol{d}^*\cdot\boldsymbol{e}_z)}{c^3} = \frac{d_0^2}{c^3}. \tag{24}$$

The exciton dispersion would be

$$E^0_{\boldsymbol{k}} = E_0 + 2t_x\cos(k_x a) + 2t_y\cos(k_y a) + 2t_z\cos(k_z c). \tag{25}$$

Thus we have the exciton bandwidths

$$B_\perp = -8t_x = -8t_y = 4d_0^2/a^3,\ B_z = 4t_z = 4d_0^2/c^3, \tag{26}$$

which is Eq. (6) of the main text.

5 Evaluation of Green's function

Here we evaluate the exciton Green's function,

$$G^0(0,E) = \frac{1}{N}\sum_{\boldsymbol{k}} \frac{1}{E - E^0_{\boldsymbol{k}}}. \tag{27}$$

We denote $k'_x = k_x a$, $k'_y = k_y a$, and $k'_z = k'_z c$, and express the Green's function as

$$G^0(0,E) = \frac{1}{8\pi^3}\int_{-\pi}^{\pi} dk'_x \int_{-\pi}^{\pi} dk'_y \int_{-\pi}^{\pi} dk'_z \frac{1}{(E - \frac{B_\perp}{2} - \frac{B_z}{2}) - \frac{1}{2}B_z\cos k'_z + \frac{B_\perp}{2}\cos\frac{k'_x+k'_y}{2}\cos\frac{k'_x-k'_y}{2}}. \tag{28}$$

By introducing variables $x = \frac{k'_x+k'_y}{2}$ and $y = \frac{k'_x-k'_y}{2}$, the integration of x and y in Eq. (28) can be worked out first, which has the form

$$\begin{aligned} I_1 &\equiv \int_{-\pi}^{\pi} dk'_x \int_{-\pi}^{\pi} dk'_y \frac{1}{A - B\cos\frac{k'_x+k'_y}{2}\cos\frac{k'_x-k'_y}{2}} \\ &= \int_{-\pi/2}^{\pi/2} dx \int_{-\pi/2}^{\pi/2} dy \frac{4}{A - B\cos x\cos y}. \end{aligned} \tag{29}$$

Using

$$\int_0^{\pi} dy \frac{1}{A' - B'\cos y} = \frac{\pi}{\sqrt{A'^2 - B'^2}}, \tag{30}$$

we have

$$I_1 = 4\pi\int_{-\pi/2}^{\pi/2} dx \frac{1}{A\sqrt{1 - \frac{B^2}{A^2}\cos^2 x}} = \frac{4\pi}{A}K(B/A), \tag{31}$$

where $K(x)$ is the complete elliptic integral of the first kind. Thus we have the result displayed in the main text,

$$\begin{aligned} G^0(0,E) &= -\frac{4}{\pi^2}\int_0^{\pi/2} dk_z \Big[\frac{1}{B_\perp + B_z[1-\cos(k_z c)] - 2E} K\Big(\frac{B_\perp}{B_\perp + B_z[1-\cos(k_z c)] - 2E}\Big) \\ &+ \frac{1}{B_\perp + B_z[1+\cos(k_z c)] - 2E} K\Big(\frac{B_\perp}{B_\perp + B_z[1+\cos(k_z c)] - 2E}\Big). \end{aligned} \tag{32}$$

6 Bandwidths in the presence of out-of-plane tilting

In the presence of an out-of-plane tilt, two adjacent PbX_6 octahedra within a layer have $\theta_1 = -\theta_2 = \theta$, $\phi_1 = -\phi_2 = \phi$, while those across layers have $\theta_1 = \theta_2 = \theta$, $\phi_1 = \phi_2 = \phi$. The two adjacent PbX_6 octahedra within a layer then have transition dipoles

$$\boldsymbol{d}_1 = d_0\Big(\frac{1+\cos\theta}{2}e^{i\phi}\boldsymbol{e}_+ + \frac{1-\cos\theta}{2}e^{-i\phi}\boldsymbol{e}_- + \frac{1}{\sqrt{2}}\sin\theta\boldsymbol{e}_z\Big), \tag{33}$$

$$\boldsymbol{d}_2 = d_0\Big(\frac{1+\cos\theta}{2}e^{-i\phi}\boldsymbol{e}_+ + \frac{1-\cos\theta}{2}e^{i\phi}\boldsymbol{e}_- - \frac{1}{\sqrt{2}}\sin\theta\boldsymbol{e}_z\Big). \tag{34}$$

The strengths of dipole-dipole interaction along the x-, y-, and z-axis are

$$\begin{aligned} t_x &= \frac{\boldsymbol{d}_1\cdot\boldsymbol{d}_2^*}{a^3} - 3\frac{(\boldsymbol{d}_1\cdot\boldsymbol{e}_x)(\boldsymbol{d}_2^*\cdot\boldsymbol{e}_x)}{a^3} \\ &= -\frac{1}{4}(\cos^2\theta+1)\cos 2\phi + \frac{1}{4}\sin^2\theta - \frac{1}{2}i\cos\theta\sin 2\phi, \end{aligned} \tag{35}$$

$$\begin{aligned} t_y &= \frac{\boldsymbol{d}_1\cdot\boldsymbol{d}_2^*}{a^3} - 3\frac{(\boldsymbol{d}_1\cdot\boldsymbol{e}_y)(\boldsymbol{d}_2^*\cdot\boldsymbol{e}_y)}{a^3} \\ &= -\frac{1}{4}(\cos^2\theta+1)\cos 2\phi - \frac{1}{4}\sin^2\theta - \frac{1}{2}i\cos\theta\sin 2\phi, \end{aligned} \tag{36}$$

$$\begin{aligned} t_z &= \frac{\boldsymbol{d}_1\cdot\boldsymbol{d}_1^*}{c^3} - 3\frac{(\boldsymbol{d}_1\cdot\boldsymbol{e}_z)(\boldsymbol{d}_1^*\cdot\boldsymbol{e}_z)}{c^3} \\ &= \frac{d_0^2}{c^3}\Big(1-\frac{3}{2}\sin^2\theta\Big). \end{aligned} \tag{37}$$

Since t_x and t_y are complex while t_z is real, the corresponding intra-band widths for small θ are

$$B_\perp = 8|t_x t_x^*|^{1/2} = 8|t_y t_y^*|^{1/2} \simeq 4\frac{d_0^2}{a^3}\cos^2\theta,\ B_z = 4t_z = \frac{4d_0^2}{c^3}\Big(1-\frac{3}{2}\sin^2\theta\Big), \tag{38}$$

which are the results displayed in Eq. (14) of the main text.

7 Justification of parameter values

We can estimate the ODP strength and exciton bandwidths using typical material properties of 2D HOIPs. If we choose $l_\mathrm{a} = 6$ Å, $m_\mathrm{e} = 0.291m$, $m_\mathrm{h} = 0.321m$[6], from

$$A = -\frac{\pi\hbar^2}{l_\mathrm{a}^3}\Big(\frac{1}{m_\mathrm{e}}+\frac{1}{m_\mathrm{h}}\Big) + Z^*\frac{\varepsilon_a-\varepsilon_b}{\varepsilon(l_\mathrm{a}+l_\mathrm{b})}, \tag{39}$$

we have $A = -0.76$ eV/Å if we neglect the third term, which, for a binding energy of 200 meV and $l_\mathrm{b} = 2l_\mathrm{a}$, would be about 0.01 eV/Å. The strength γ frequently used in the main text is $\gamma = -A(\hbar/M\Omega)^{1/2}$. By using $\hbar\Omega_\mathrm{s} = 14$ meV, $\gamma = 0.037$ eV for Pb-I layers and 0.047 eV for Pb-Br ones. Since the effective-masses of electron and hole, according to different first-principles calculations, can be as small as $0.10m$, γ may reach 0.1 eV.

The transition dipole strength can be estimated from the oscillator strength,

$$d_0^2 = \frac{e^2\hbar^2 f_\perp}{2mE_\mathrm{g}},\ B_\perp = 4d_0^2/a^3. \tag{40}$$

Using the band gap $E_\mathrm{g} = 2.5$ eV and the oscillator strength of $(C_{10}H_{21}NH_3)_2PbI_4$[7], $B_\perp = 4d_0^2/a^3 = 0.2$ eV. The values of γ and $B_\perp$ used in the main text are based on the above estimates.

8 Exciton bandwidths in corrugated 2D HOIPs

In the corrugated 2D structure displayed in Fig. 5 of the main text, the arrangement of PbX_6 octahedra along the x-axis is the same as in the flat one. Thus the strength of dipole-dipole interaction along the x-axis, for $\boldsymbol{d} = d_0\boldsymbol{e}_+$, is

$$t_x = \frac{\boldsymbol{d}\cdot\boldsymbol{d}^*}{a^3} - 3\frac{(\boldsymbol{d}\cdot\boldsymbol{e}_x)(\boldsymbol{d}^*\cdot\boldsymbol{e}_x)}{a^3} = -\frac{d_0^2}{2a^3}, \tag{41}$$

where a is the center-to-center distance between adjacent PbX_6 octahedra. The arrangement of PbX_6 octahedra along the y-axis, however, differs from that in the flat one. In particular, the displacement between adjacent octahedra, $\boldsymbol{R}_{ij} = \frac{a}{\sqrt{2}}(\boldsymbol{e}_y \pm \boldsymbol{e}_z)$, have an angle of $\pi/4$ against the y axis. Consequently, the strength of dipole-dipole interaction along the y-axis becomes

$$t_y = \frac{\boldsymbol{d}\cdot\boldsymbol{d}^*}{a^3} - 3\frac{(\boldsymbol{d}\cdot\boldsymbol{R}_{ij})(\boldsymbol{d}^*\cdot\boldsymbol{R}_{ij})}{a^3} = \frac{d_0^2}{4a^3} = -\frac{1}{2}t_x. \tag{42}$$

Thus the bandwidth along the y-axis is only one half of that along the x-axis in the corrugated structure.

In the main text, instead of evaluating the Green's function in Eq. (9) of the main text using different t_x and t_y, we apply the results obtained for $t_x = t_y$ to the corrugated structure with an effective $B_\perp$. We consider two cases: One has $B_\perp = 8\sqrt{|t_x t_y|}$ and the other has $B_\perp = 8|t_y|$, which should set the upper and lower limits of the STE's energy in the corrugated structure, for the smaller one of t_x and t_y controls the onset of STE.

9 X-Pb-X stretching in 2D structures

In 2D HOIPs, a Pb-X layer can be considered as a perfect quantum well (QW) with its thickness determined by the distance between two apical X atoms in a PbX_6 octahedron. Vibration of the two X atoms normal to the Pb-X layer will alter the QW's thickness and shifts the quantized electron and hole energies in the QW. The normal modes of the X atoms' motion can be analyzed by considering the three-atom chain, X-Pb-X, perpendicular to the Pb-X layer. The three-atom vibration problem can be readily solved and the results are particularly simple if we include only the nearest-neighbor coupling between X and Pb. If we denote K^* as the spring constant of the Pb-X bond and $M_{\mathrm{X(Pb)}}$ as the mass of an X (Pb) atom, the three eign modes of this X-Pb-X chain are: an acoustic mode (Mode 1) in which the three atoms moving to the same direction with $\omega_1 = 0$, an optical mode (Mode 2) in which the central Pb is stationary and the two X atoms move out-of-phase with frequency of $\omega_2 = \sqrt{K^*/M_{\mathrm{X}}}$, and an optical mode (Mode 3) in which the two X atom move in-phase and the central Pb move toward one of X atoms while keeping the center-of-mass of the three atoms fixed, with frequency of $\omega_3 = \sqrt{K^*\left(\frac{1}{M_{\mathrm{X}}} + \frac{2}{M_{\mathrm{Pb}}}\right)}$. The three modes are displayed in Fig. 1.

Optical mode 2, i.e., the B_{1g} mode, induces no electric field but changes the thickness of the Pb-X QW, leading to a strong ODP coupling to excitons in 2D HOIPs. Optical mode 3 generates an electric field and a polar coupling to electron and hole. However, it does not alter the thickness of Pb-X QWs, and therefore couples minimally to excitons in 2D HOIPs. Acoustic mode 1 also does not alter the thickness of Pb-X QWs.

10 Coupling between excitons and acoustic phonons

Acoustic phonons can also couple to excitons. However, they do not change the QW thickness to affect the quantized electron and hole energies. Their coupling to excitons arise from modulating the

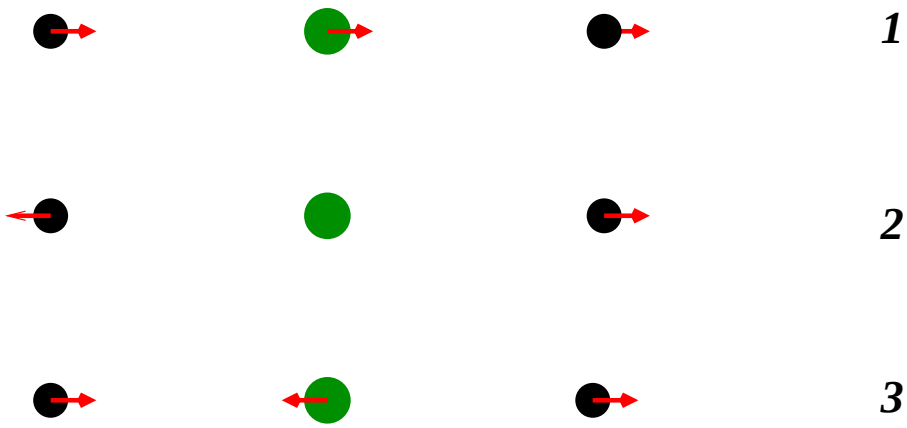

Figure 1 Eigen modes of the X-Pb-X chain. Green (black) circles represent Pb (X) ions. Red arrows indicate atomic motions in each eigen mode.

excitons' dipole-dipole coupling. If we write the exciton Hamiltonian as

$$H_{\rm ex} = \sum_i E_0 c_i^\dagger c_i + \sum_{\langle ij\rangle} t_{ij}(\boldsymbol{R}_{ij}) c_i^\dagger c_j, \tag{43}$$

acoustic motions would modify $\boldsymbol{R}_{ij}$, the distance between adjacent PbX_6 octahedra, which in turn would alter t_{ij} and give rise to an exciton-phonon coupling. Here we follow Davydov's work to obtain the exciton coupling to acoustic phonons[8]. If we denote the lattice displacement at the ith site as of $\boldsymbol{u}_i$, $\boldsymbol{R}_i = \boldsymbol{R}_i^0 + \boldsymbol{u}_i$, the exciton-phonon coupling can be written as

$$H_{\rm ac} = \sum_{\langle ij\rangle} c_i^\dagger c_j \sum_\nu \Big(u_i^\nu \frac{\partial}{\partial u_i^\nu} + u_j^\nu \frac{\partial}{\partial u_j^\nu} \Big) t_{ij}(\boldsymbol{R}_{ij}^0), \tag{44}$$

where u_i^ν ($\nu = x,y,z$) represents the ν component of $\boldsymbol{u}_i$. Expressing displacement in terms of phonon operators,

$$u_i^\nu = \sum_{s\boldsymbol{q}} \Big(\frac{\hbar}{2MN\Omega_s(\boldsymbol{q})} \Big)^{1/2} g_s^\nu (b_{\boldsymbol{q}s} + b_{-\boldsymbol{q}s}^\dagger) e^{i\boldsymbol{q}\cdot\boldsymbol{R}_i^0}, \tag{45}$$

where $\boldsymbol{g}_s$ is the eign vector of the sth mode and $\Omega_s(\boldsymbol{q})$ the phonon frequency at wavevector $\boldsymbol{q}$, and using the fact of t_{ij} depending only on $\boldsymbol{R}_{ij}$, we obtain the interaction between excitons and acoustic phonons,

$$H_{\rm ac} = \sum_{s\boldsymbol{k},\boldsymbol{q}} F_s(\boldsymbol{k},\boldsymbol{q}) c_{\boldsymbol{k}+\boldsymbol{q}}^\dagger c_{\boldsymbol{k}} (b_{\boldsymbol{q}s} + b_{-\boldsymbol{q}s}^\dagger), \tag{46}$$

where $c_{\boldsymbol{k}}^\dagger$ ($c_{\boldsymbol{k}}$) creates (destroys) an exciton with wavevector ($\boldsymbol{k}$), and

$$F_s(\boldsymbol{k},\boldsymbol{q}) = \sum_{\nu,j} e_s^\nu(\boldsymbol{q}) \Big(\frac{\hbar}{2MN\Omega_s(\boldsymbol{q})} \Big)^{1/2} \Big(\frac{\partial}{\partial u_0^\nu} + e^{i\boldsymbol{q}\cdot\boldsymbol{R}_{0j}^0} \frac{\partial}{\partial u_j^\nu} \Big) t_{0j} e^{i\boldsymbol{k}\cdot\boldsymbol{R}_{0j}^0}. \tag{47}$$

Since the exciton's dipole-dipole coupling in 2D HOIPs has been evaluated in Sec. I,

$$t_{0j}^x = -\frac{d_0^2}{2|\boldsymbol{R}_{\pm\boldsymbol{x}} - \boldsymbol{R}_0|^3},\ t_{0j}^y = -\frac{d_0^2}{2|\boldsymbol{R}_{\pm\boldsymbol{y}} - \boldsymbol{R}_0|^3},\ t_{0j}^z = \frac{d_0^2}{2|\boldsymbol{R}_{\pm\boldsymbol{z}} - \boldsymbol{R}_0|^3}, \tag{48}$$

where $\boldsymbol{R}_{\pm\boldsymbol{q}}$ is the two neighboring sites of $\boldsymbol{R}_0$ along the $\pm\boldsymbol{e}_q$ ($q = x,y,z$) direction, Eq. (34) can be readily evaluated.

For $\boldsymbol{k}||\boldsymbol{q}||\boldsymbol{e}_x$, $\boldsymbol{k}||\boldsymbol{q}||\boldsymbol{e}_y$, only the longitudinal acoustic phonons contribute to the exciton-phonon coupling,

$$\begin{aligned} F(\boldsymbol{k},\boldsymbol{q}) &= -12i\Big(\frac{\hbar}{2MN\Omega_s(\boldsymbol{q})}\Big)^{1/2} t_x \cos\Big(ka+\frac{qa}{2}\Big)\sin\Big(\frac{qa}{2}\Big) \\ &= i\frac{3}{4}\Big(\frac{\hbar a}{NMv_\perp}\Big)^{1/2}\frac{B_\perp}{a}\cos\Big[\Big(k+\frac{q}{2}\Big)a\Big]\sqrt{\sin\Big(\frac{qa}{2}\Big)} \\ &\simeq i\frac{3}{4}\Big(\frac{\hbar}{NMv_\perp a}\Big)^{1/2} B_\perp \cos\Big(\frac{qa}{2}\Big)\sqrt{\sin\Big(\frac{qa}{2}\Big)} \end{aligned} \tag{49}$$

Here we have assumed $ka \ll 1$ because exciton density is not very high and mostly is localized around $k \sim 0$ and used the acoustic phonon dispersion,

$$\Omega_l(q) = \frac{v_\perp}{a}\sin\frac{qa}{2}, \tag{50}$$

with $v_\perp$ being the intra-layer speed of sound. Similarly for $\boldsymbol{k}||\boldsymbol{q}||\boldsymbol{e}_z$, the longitudinal acoustic phonon has a dispersion of $\Omega_l(q) = \frac{v_z}{c}\sin\frac{qc}{2}$ (v_z being the inter-layer speed of sound, and contributes to the exciton-phonon coupling,

$$F(0,\boldsymbol{q}) \simeq -i\frac{3}{2}\Big(\frac{\hbar}{NMv_z c}\Big)^{1/2} B_z \cos\Big(\frac{qc}{2}\Big)\sqrt{\sin\Big(\frac{qc}{2}\Big)}, \tag{51}$$

The calculated $V_{\rm ac}(\boldsymbol{q}) \equiv F(0,\boldsymbol{q})$ is plotted in Fig. 1b. The measured intra-layer and inter-layer Young's moduli of $(C_4H_9NH_3)_2PbI_4$ are $c_{\rm intra} = 11.2 \pm 1.4$ GPa[9] and$c_{\rm inter} = 3.3 \pm 0.1$ GPa[10]. The speed of sound can be obtained from the Young's modulus, $v_\perp = \sqrt{c_{\rm intra}/\rho}$ and $v_z = \sqrt{c_{\rm inter}/\rho}$, where $\rho \equiv NM$ is the material's mass density. For $\rho = 2.5$ g/cm^3, we have $v_\perp = 2.1\times10^5$ cm/s and $v_z = 1.1\times10^5$ cm/s, which are consistent with the observed speeds of sound along and across Pb-X layers[11]. Using these parameters, an upper bound of the exciton bandwidth $B_\perp = 0.4$ eV, and $c = 2.5a$, we find that $V_{\rm ac}(\boldsymbol{q})$ is orders-of-magnitude weaker than the ODP. Thus we can safely neglected the acoustic phonons in studying STEs in 2D HOIPs.

References

[1] Z. G. Yu, *Sci. Rep.*, 2016, **6**, 28576.

[2] Z.-G. Yu, *J. Phys. Chem. Lett.*, 2017, **9**, 1–7.

[3] Z.-G. Yu, *J. Phys. Chem. Lett.*, 2016, **7**, 3078–3083.

[4] Z.-G. Yu, *J. Phys. Chem. C*, 2017, **121**, 3156–3160.

[5] R. S. Knox, *Theory of Excitons*, Academy Press, 1963.

[6] D. Wang, B. Wen, Y.-N. Zhu, C.-J. Tong, Z.-K. Tang and L.-M. Liu, *J. Phys chem. Lett.*, 2017, **8**, 876–883.

[7] T. Ishihara, J. Takahashi and T. Goto, *Phys. Rev. B*, 1990, **42**, 11099–11107.

[8] A. S. Davydov, *Theory of Molecular Excitons*, Plenum Press, 1971.

[9] Q. Tu, I. Spanopoulos, P. Yasaei, C. Stoumpos, M. G. Kanatzidis, G. S. Shekhawat and V. P. Dravid, *arXiv:1806.04835*, 2018.

[10] Q. Tu, I. Spanopoulos, S. Hao, C. Wolverton, M. G. Kanatzidis, G. S. Shekhawat and V. P. Dravid, *ACS Appl. Mater. Interfaces*, 2018, **10**, 22167–22173.

[11] P. Guo, C. C. Stoumpos, L. Mao, S. Sadasivam, J. B. Ketterson, P. Darancet, M. G. Kanatzidis and R. D. Schaller, *Nat. Commun.*, 2018, **9**, 2019.